PNAS
www.pnas.org

Supplementary Information for

$G_{q/11}$-dependent regulation of endosomal cAMP generation by parathyroid hormone class B GPCR

Alex D. White[1,2,†], Frederic G. Jean-Alphonse[1,†,#], Fei Fang[1], Karina A. Peña[1], Shi Liu[4], Gabriele M. Konig[5], Asuka Inoue[6], Despoina Aslanoglou[3], Samuel H. Gellman[4], Evi Kostenis[5], Kunhong Xiao[1], and Jean-Pierre Vilardaga[1,*]

[1]Department of Pharmacology and Chemical Biology, [2]Graduate Program in Molecular Pharmacology, and [3]Department of Psychiatry, School of Medicine, University of Pittsburgh, Pittsburgh, PA 15261, USA; [4]Department of Chemistry, University of Wisconsin-Madison, WI 53706, [5]Molecular, Cellular and Pharmacobiology Section, Institute of Pharmaceutical Biology, University of Bonn, Bonn, Germany; [6]Graduate School of Pharmaceutical Sciences, Tohoku University, Sendai, Miyagi 980-8578, Japan.

[†]Contributed equally to this study.

[#]Present address: Unité de la Physiologie de la Reproduction et des Comportements, INRA, CNRS, 37380 Nouzilly, France.

*Jean-Pierre Vilardaga
Email: jpv@pitt.edu

This PDF file includes:

Supplementary text
Figures S1 to S7
Table S1

www.pnas.org/cgi/doi/10.1073/pnas.1918158117

Supplementary Information Text

Method

Stable Isotope Labeling by Amino acids in Cell culture (SILAC). The HEK-293 wild-type and $G_{q/11}^{KO}$ cell lines stably expressing the recombinant HA-tagged human PTHR (HA-PTHR) were generated and hereafter referred to as PTHR-WT and PTHR-$G_{q/11}^{KO}$ cells, respectively. The HA-PTHR-WT cells were cultured in SILAC "light" medium and the PTHR-$G_{q/11}^{KO}$ cells in SILAC "heavy" medium. The SILAC media were prepared from custom-ordered DMEM powder without arginine, lysine, and leucine (Gibco, formula # 03-5080EB) (Gibco/Invitrogen). [$^{13}C_6$, $^{15}N_2$]-L-lysine (50 mg/liter) and [$^{13}C_6$,$^{15}N_4$]-L-arginine (25 mg/liter) (Cambridge Isotope Laboratories) were added to the "Heavy" medium, whereas equal concentrations of conventional lysine and arginine were added to the "Light" medium. All "Light" and "Heavy" media were supplemented with L-leucine (104 mg/liter), L-proline (10 mg/liter), 10% dialyzed FBS (Hyclone) (Thermo Scientific), 1% penicillin/streptomycin, and G418 (150 mg/ml). These two pools of cell lines were cultured in SILAC media side-by-side for more than six doublings until the isotope incorporation rates in "Heavy" cells were higher than 95%. The two SILAC cell pools were then each expanded to 10 culture dishes of 150-mm diameter. When the cells reached ~80% confluence, they were serum-starved for 4 hours. To quantitatively compare the phosphorylation events (sites and extents of phosphorylation) on the PTHR in WT and $G_{q/11}^{KO}$ conditions, both pools of cells were stimulated with 200 nM PTH(1–34) for 5 min before harvesting. The "Light" and "Heavy" labeled cells were then harvested separately and subjected receptor isolation.

HA-PTHR isolation, digestion and peptide desalting. The lightly and heavily labeled HA-PTHR were isolated separately from "light" SILAC cells and "heavy" SILAC cells using Pierce™ Anti-HA Agarose beads (Catalog number: 26181, Thermo Fisher Scientific). Briefly, crude membrane fractions were prepared from harvested cells as previously described (1, 2). Labeled HA-PTHR was then extracted from crude membrane preparations with 1× buffer [20 mM tris-HCl (pH 8.0), 100 mM NaCl, and 2 mM EDTA] containing 1% DDM (n-dodecyl b-D-maltoside), protease inhibitors and phosphatase inhibitors. HA-PTHR were isolated from the extraction solution by incubating with 200 µL Pierce™ Anti-HA Agarose beads with rotation at 4 °C for 4 hours. The HA-PTHR bound anti-HA Agarose beads were washed with 1× buffer containing 0.1% DDM five times, and

then eluted with 100 µL 2X SDS-PAGE buffer (containing 10 mM dithiothreitol (DTT)) by incubating at 37 °C for 1 hour. The receptor proteins were alkylated with 30 mM iodoacetamide (IAA) in the dark at room temperature for 30 min. After receptor isolation, same amounts of lightly and heavily labeled HA-PTHR were mixed before subjected to SDS-PAGE separation. The protein bands corresponding to HA-PTHR were excised from SDS-PAGE gel for in-gel protein digestion.

Tryptic digestion of HA-PTHRs was performed as previously described (3, 4). In brief, the excised gel bands were chopped into small pieces and destained by distaining solution (50 mM ammonium bicarbonate in 50% acetonitrile). Sequence grade trypsin (10 ng/ µL, modified, Promega) in 50 mM NH4HCO3 (pH 8.0) was then added to the tubes to cover the destained gel pieces. The tryptic digestion reactions were incubated at 37 °C for overnight. An equal volume of 100% acetonitrile (CH_3CN) was added to the digested gel samples for peptide extraction and repeated for three times. The extracted peptides were pooled into a pre-washed protein LoBind tube (Catalog number: 13698793, Fisher) and then dried under vacuum on a SpeedVac evaporator. The peptide samples were desalted with handmade Stage Tips as previously described (3). The desalted peptides were lyophilized with a SpeedVac evaporator, reconstituted in 0.1% trifluoroacetic acid, 2% acetonitrile, and 25 mM citrate, and subjected to LC-MS/MS analysis.

MS and data analyses. LC-MS/MS analyses were performed on a Thermo Scientific LTQ Orbitrap Velos mass spectrometer (Thermo Fisher) with a Finnigan Nanospray II electrospray ionization source. The peptide samples were loaded onto a nanoViper Compatible PicoChip Column (Catalog number: 1PCH7515-105H354-NV, New Objective) and separated with a Waters nanoACQUITY UPLC System. Instrument control and primary data processing were done with the Xcalibur software package. The LTQ Orbitrap Velos was operated in data-dependent mode using a TOP10 strategy (5). MS/MS spectra were searched with the SEQUEST algorithm against a composite database containing the human HA-PTHR sequence or HA-PTHR with its interacting proteins, as well as their reverse sequences. Search parameters allowed for three missed tryptic cleavages, a mass tolerance of ± 80 parts per million (ppm), a static modification of 57.02146 daltons (carboxyamidomethylation) on cysteine, and up to eight total dynamic modifications: 79.96633 daltons (phosphorylation) on Serine, Threonine, and Tyrosine; 15.99491 daltons (oxidation) on Methionine; 6.02012 daltons or 10.00827 daltons on Arginine; and 4.00709 daltons or 8.01420 daltons on Lysine. Search results were filtered to include < 1% matches

to reverse sequences by restricting the mass tolerance window, and setting thresholds for Xcorr and dCn′ (defined as the normalized difference between Xcorr values of the top-ranked candidate peptide and the next candidate with a different amino acid sequence). Matches for phosphopeptides were validated manually with special consideration of intense fragment ions formed through cleavage N-terminal to Proline residues and neutral losses of phosphoric acid. Peptide quantification was performed with the Vista program (6) as well as by manual calculation with Qual Browser (version 3.0.63). In brief, the theoretical mass of “Light” and “Heavy” variants of each peptide was calculated and used to identify ion peaks in the high mass accuracy precursor scans for each. The intensity of the peaks was used to construct ion chromatograms. For each isotopic variant, the peak height and background-subtracted area under the curve were used to calculate the “Heavy”-to-“Light” ($G_{q/11}^{KO}$:WT) abundance ratios. Since isomeric singly phosphorylated peptides (^{489}SGSSSYSYGPM*VSHTSVTNVGPR^{511}) with phosphorylation at different positions co-eluted from LC column during chromatographic separation, the quantitative analysis reflects a summary of a mixture of these co-eluted singly phosphorylated peptides.

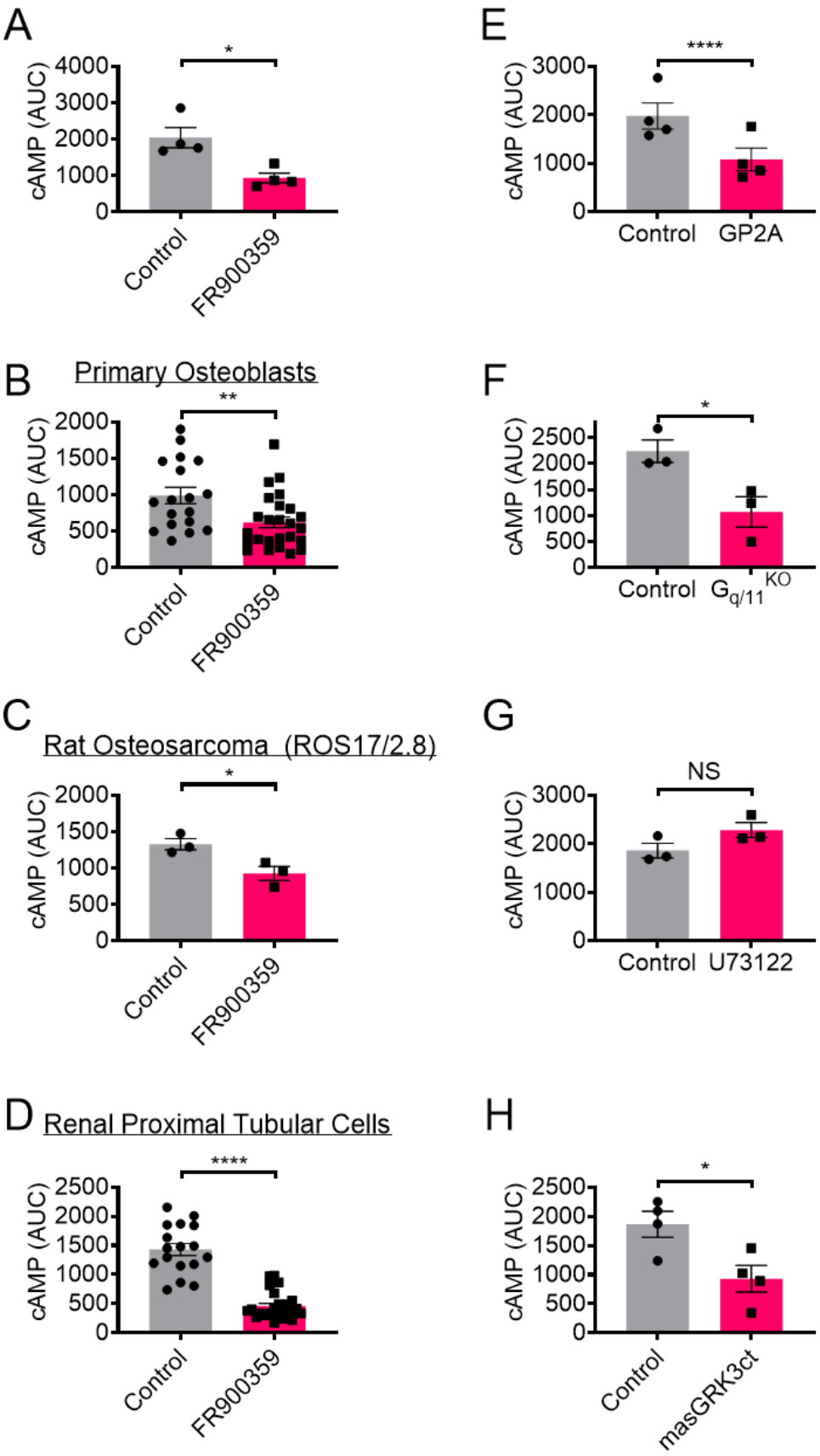
A
cAMP (AUC)
4000
3000
2000
1000
0
*
Control
FR900359
B
Primary Osteoblasts
cAMP (AUC)
2000
1500
1000
500
0
**
Control
FR900359
C
Rat Osteosarcoma (ROS17/2.8)
cAMP (AUC)
2000
1500
1000
500
0
*
Control
FR900359
D
Renal Proximal Tubular Cells
cAMP (AUC)
2500
2000
1500
1000
500
0
****
Control
FR900359
E
cAMP (AUC)
3000
2000
1000
0
****
Control
GP2A
F
cAMP (AUC)
2500
2000
1500
1000
500
0
*
Control
Gq/11KO
G
cAMP (AUC)
3000
2000
1000
0
NS
Control
U73122
H
cAMP (AUC)
2500
2000
1500
1000
500
0
*
Control
masGRK3ct

Fig. S1. Statistical analysis for cAMP time-course experiments in Figure 1. **Fig. S1. Statistical analysis for cAMP time-course experiments in Figure 1**. (A–H) Bars represent the time integrated cAMP responses determined by measuring the area under the curve from 0 to 30 min of time courses shown in Figure 1A–H. Statistical analysis was performed by a *t*-test (**P* < 0.05; ***P* < 0.01; *****P* < 0.0001).

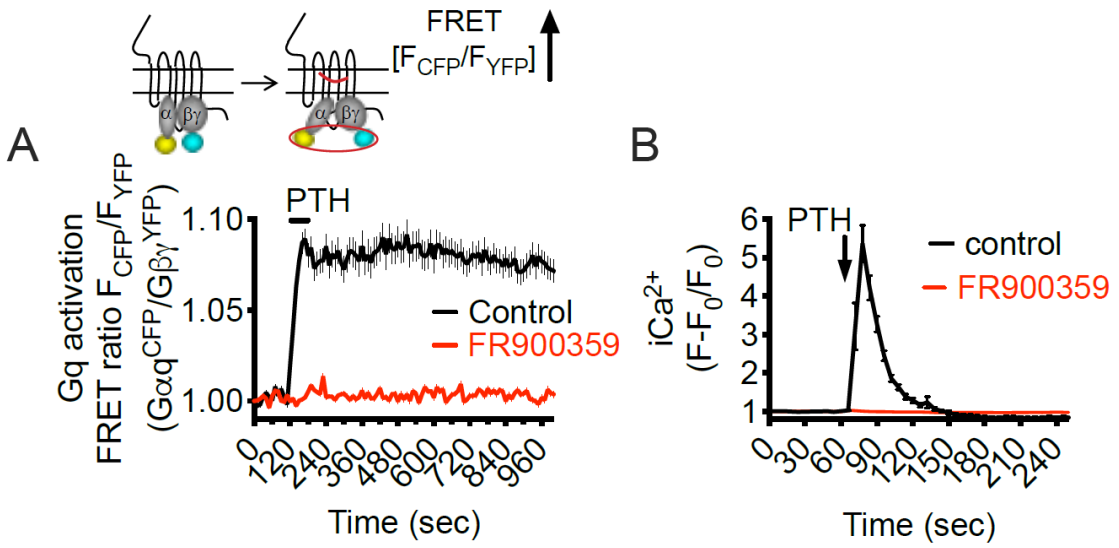

Fig. S2. Effect of FR900359 on PTH-mediated $G_{q/11}$ signaling. (A) The scheme represents the approach used to record kinetics of $G_{q/11}$ activation based on changes in FRET between CFP-labeled $G\alpha_q$ and YFP-labeled Gβγ subunits. On agonist exposure, a fast increase in the FRET ratio F_{CFP}/F_{YFP} indicates activation of Gq. The plot shows averaged time courses of Gq activation measured in single HEK-293 cells co-expressing PTHR and the FRET-based Gq with the initial value of FRET ratio at t = 0 set to 1. The horizontal bar represents the duration of PTH (100 nM) application. Data represent the mean value ± s.e.m. of *N* = 3 experiments and *n* = 9 cells (control) and 17 cells (FR900359, 1 μM). (B) Changes in the intracellular levels of Ca^{2+} in response to 100 nM PTH were measured by epifluorescence following of the calcium sensor R-Geco1.2 and imaging at 561 nm excitation and 581 emission with or without FR900359. Traces are representative of three independent experiments and *n* = 33 (control) and *n* = 18 (FR900359, 1 μM) cells.

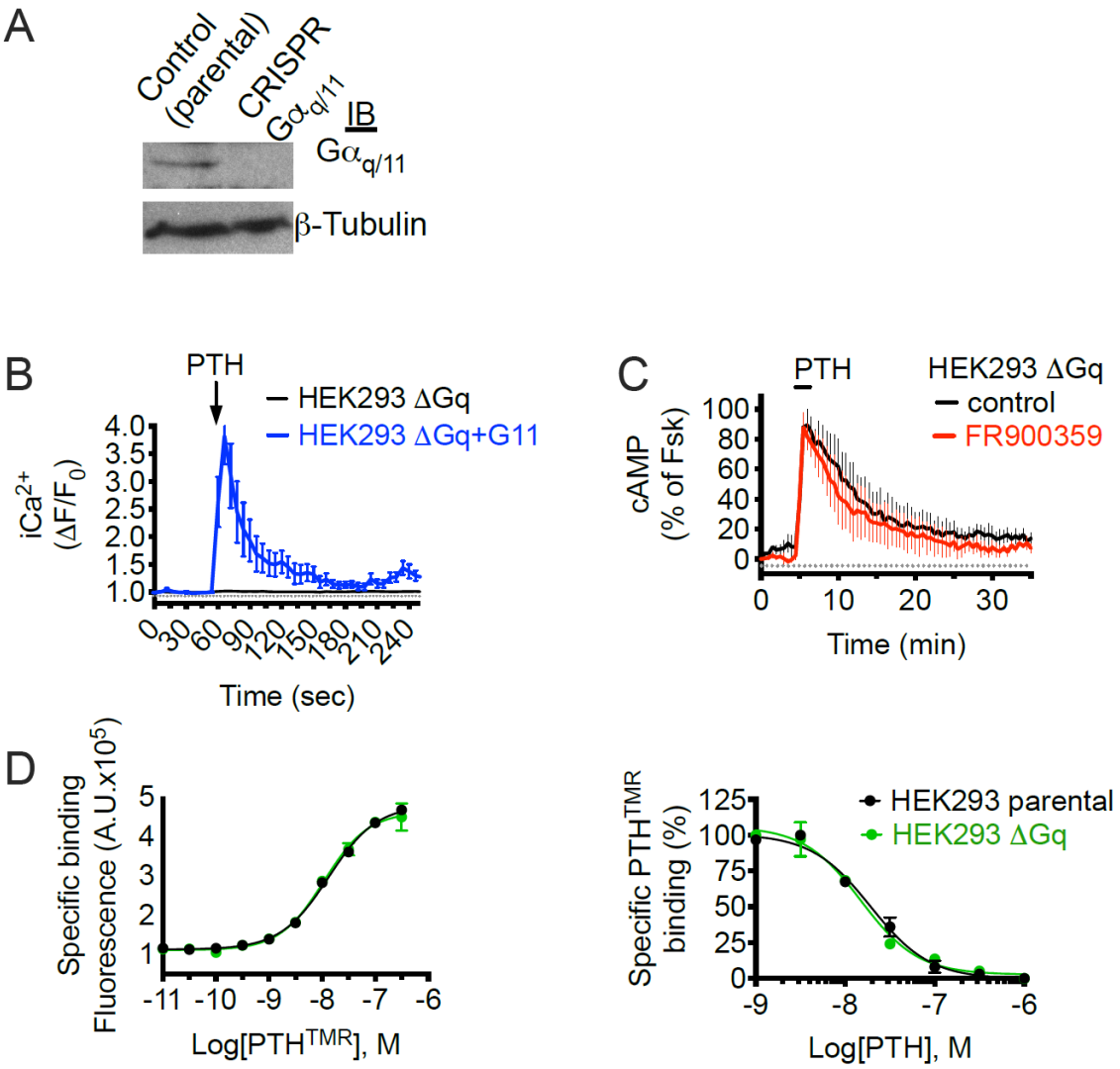

Fig. S3. PTH signaling and binding in HEK293 cells with $G_{q/11}$ knockout via CRISPR. (A) Expression of $G_{q/11}$ in parental and HEK-$G_{q/11}^{KO}$ cells expressing the recombinant PTHR and using an anti-$G\alpha_{q/11}$ antibody and anti β-tubulin for loading control. (B) Intracellular Ca^{2+} mobilization measurements in HEK-$G_{q/11}^{KO}$ transfected with or without $G\alpha_{11}$. (C) Time courses of PTH-induced cAMP production in HEK-$G_{q/11}^{KO}$ cells without (control, black) or with FR900359 (red). (D) Saturation (left) and competition (right) binding isotherm experiments in HEK parental or HEK-$G_{q/11}^{KO}$ stably expressing PTHR. Data represent the mean ± s.e.m. of *N* = 3 experiments.

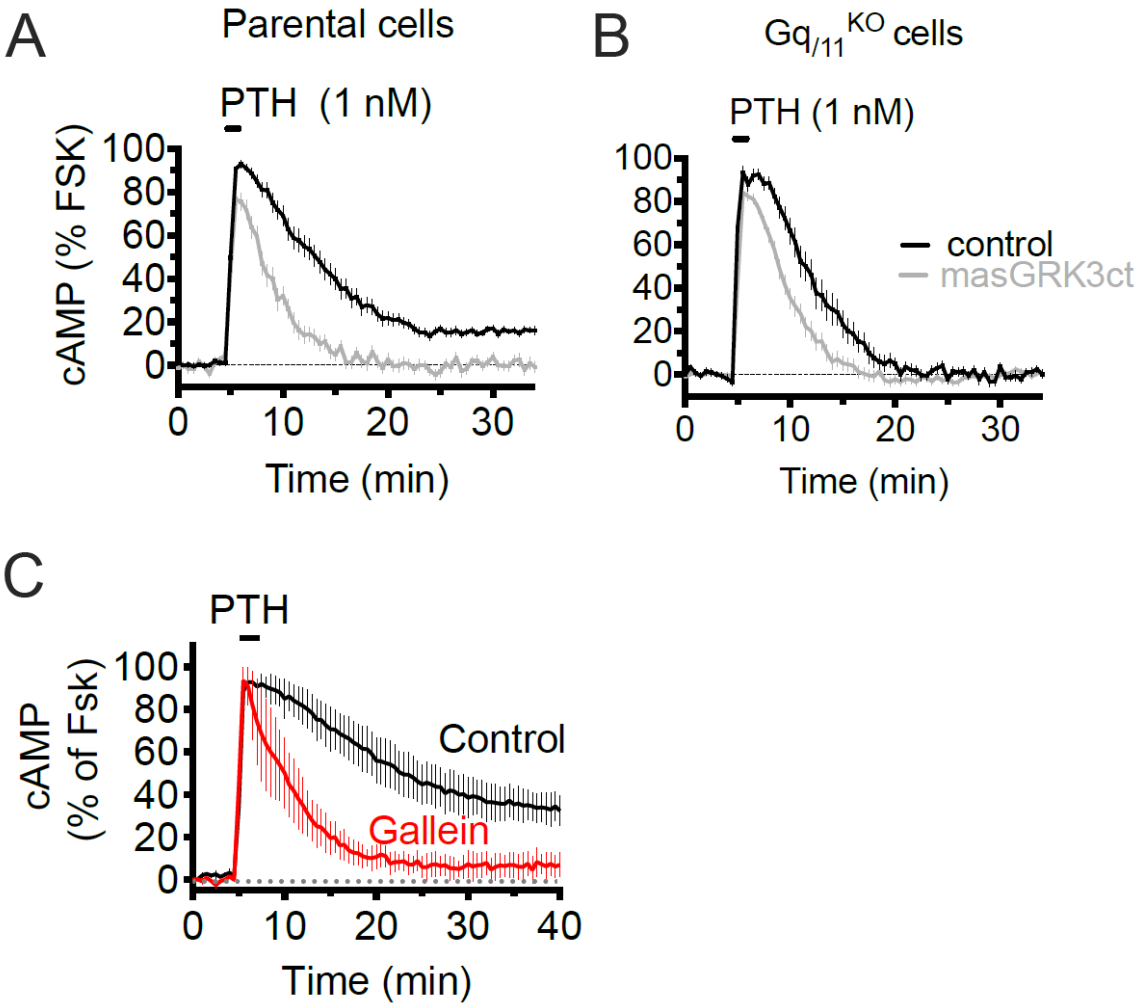

Fig. S4. Regulation of cAMP responses by $G_{q/11}$-derived cell surface Gβγ. (A, B) Time courses of cAMP upon exposure to 1 nM PTH in parental or $G_{q/11}^{KO}$ cells transiently expressing PTHR +/- masGRK3ct. (C) Similar experiments in HEK-PTHR cells stimulated with 10 nM PTH +/- the Gβγ inhibitor gallein (30 μM). Data represent the mean ± s.e.m. of *N* = 3 experiments and *n* = 15–27 cells per experiment.

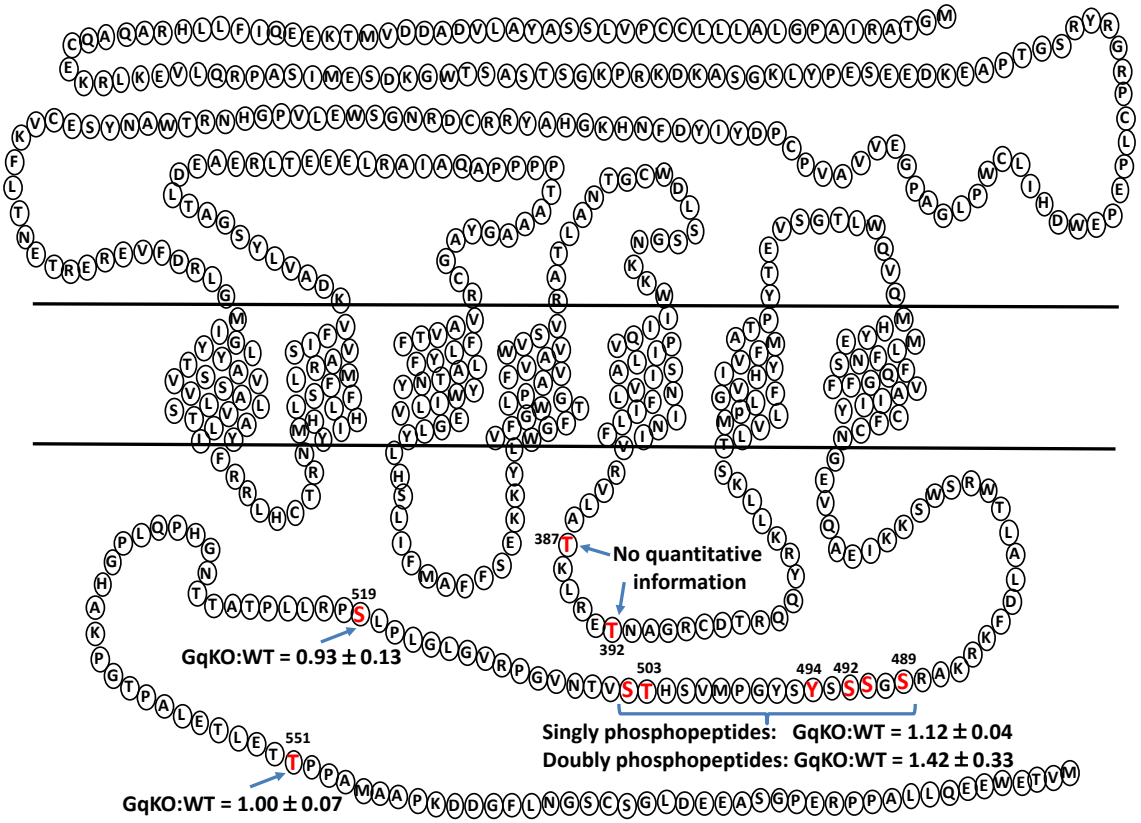

Fig. S5. SILAC-based quantitative phosphorylation analysis of PTHR. Summary of intracellular phosphorylation sites in HA-PTHR and corresponding changes in response to 200 nM PTH in wild-type or $G_{q/11}^{KO}$ cells. Phosphorylation sites were determined by LC-MS/MS and indicated in red in the snake view map of the PTHR, and normalized ratios are expressed as $G_{q/11}^{KO}$:wild-type. A comprehensive list of identified phosphopeptides is provided in Table S1.

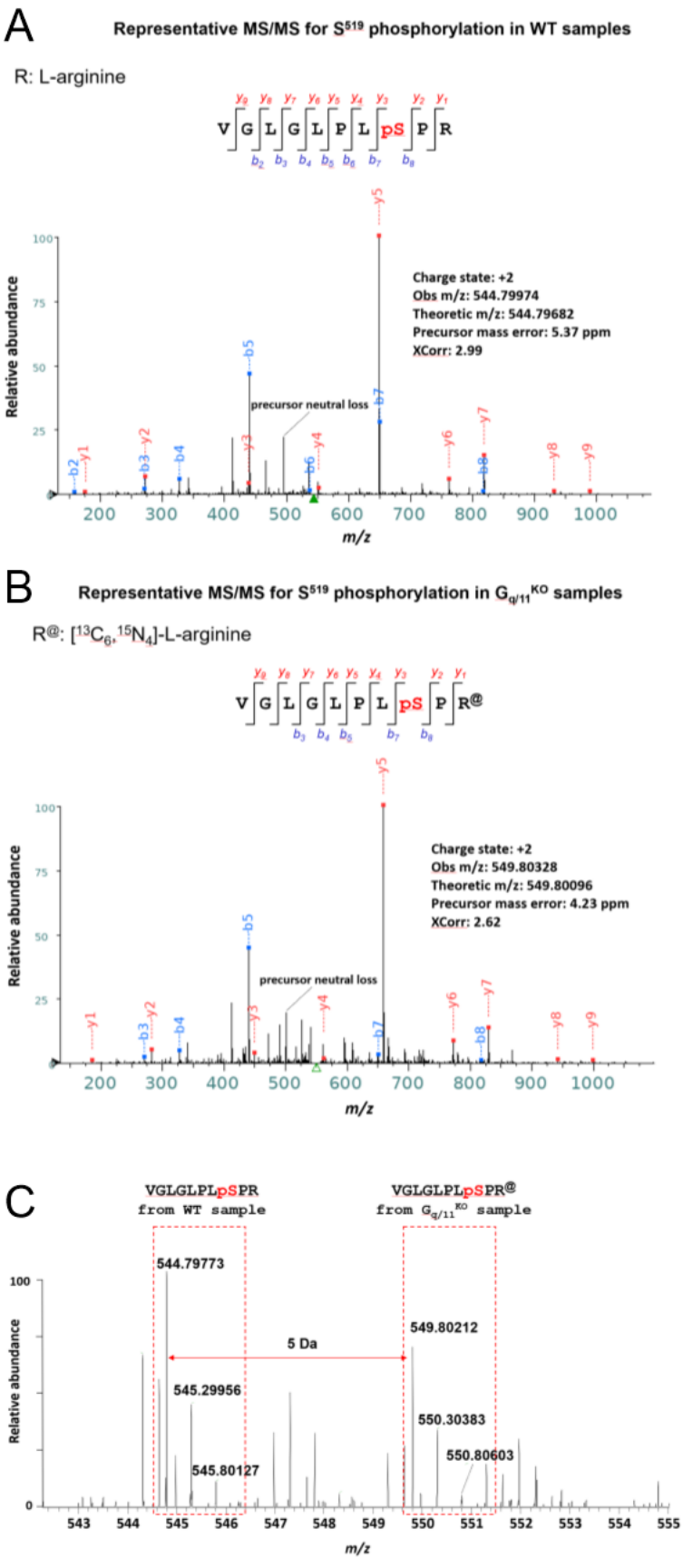
A
Representative MS/MS for S519 phosphorylation in WT samples
R: L-arginine
V G L G L P L pS P R
Charge state: +2
Obs m/z: 544.79974
Theoretic m/z: 544.79682
Precursor mass error: 5.37 ppm
XCorr: 2.99
precursor neutral loss
Relative abundance
m/z
B
Representative MS/MS for S519 phosphorylation in Gq/11KO samples
R@: [13C6,15N4]-L-arginine
V G L G L P L pS P R@
Charge state: +2
Obs m/z: 549.80328
Theoretic m/z: 549.80096
Precursor mass error: 4.23 ppm
XCorr: 2.62
precursor neutral loss
Relative abundance
m/z
C
VGLGLPLpSPR
from WT sample
VGLGLPLpSPR@
from Gq/11KO sample
544.79773
549.80212
5 Da
545.29956
550.30383
545.80127
550.80603
Relative abundance
m/z

Fig. S6. Representative MS/MS spectra of S519 phosphorylation in wild-type and $G_{q/11}^{KO}$ cells. (A, B) Annotated MS/MS fragmentation spectrum for the phosphopeptide ^{512}VGLGLPLpSPR^{521} from samples treated with 200 nM PTH in wild-type (A) or $G_{q/11}^{KO}$ cells (B) for 5 min. The peptide sequence is shown at the top of the MS/MS spectrum with phosphorylated residues highlighted in red. The identified fragmentation *y* (red color) and *b* (blue color) ions are indicated. (C) Identification of "light" (wild-type cells) and "heavy" ($G_{q/11}^{KO}$ cells) versions of the phosphopeptide ^{512}VGLGLPLpSPR^{521}. The Δ*m/z* between these peptides is 5.

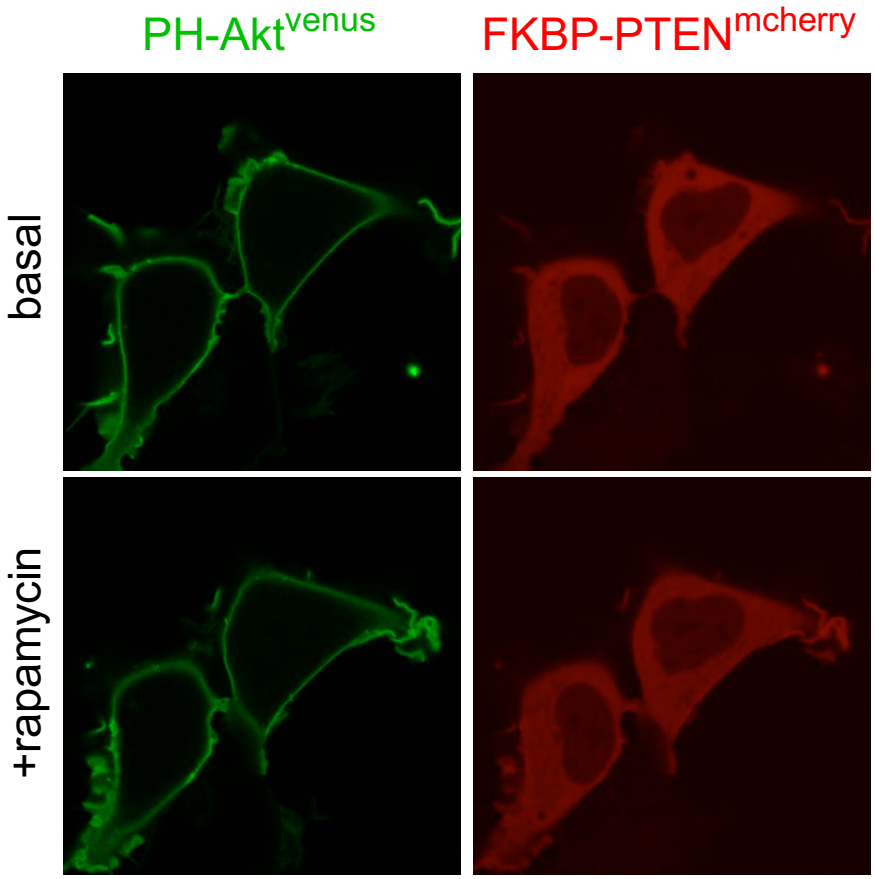

Fig. S7. PtdIns(3,4,5)P_3 unaltered by the catalytically inactive PTEN^{C124S}. Cells expressing PTHR, FRB-Lyn$_{11}$, FKBP-PTEN^{C124S}-mCherry, and PH-Akt^{venus} were treated with 1 μM rapamycin.

Table S1. List of phosphopeptide sequences and relative fold-changes

Phosphopeptides	Gq KO/WT
^{540}PGTPALETLET**pT**PPAM*AAPK^{559}	1.00±0.07
^{489}**pS**GSSSYSYGPM*VSHTSVTNVGPR^{511}	1.12±0.04
^{489}SG**pS**SSYSYGPM*VSHTSVTNVGPR^{511}	
^{489}SGS**pS**SYSYGPM*VSHTSVTNVGPR^{511}	
^{489}SGSSS**pY**SYGPM*VSHTSVTNVGPR^{511}	
^{489}SGSSSYSYGPM*VSH**pT**SVTNVGPR^{511}	
^{489}SGSSSYSYGPM*VSHT**pS**VTNVGPR^{511}	
^{489}SGS**pS**SYSYGPM*VSHT**pS**VTNVGPR^{511}	1.42±0.33
^{489}SGSSS**pY**SYGPM*VSH**pT**SVTNVGPR^{511}	
^{512}VGLGLPL**pS**PR^{521}	0.92±0.13
^{384}VLA**pT**KLRETNAGR^{396}	No quantitative information
^{384}VLATKLRE**pT**NAGR^{396}	

SI References

1. Nobles KN*, et al.* (2011) Distinct phosphorylation sites on the beta(2)-adrenergic receptor establish a barcode that encodes differential functions of beta-arrestin. *Science signaling* 4(185):ra51.
2. Xiao K & Shenoy SK (2011) Beta2-adrenergic receptor lysosomal trafficking is regulated by ubiquitination of lysyl residues in two distinct receptor domains. *The Journal of biological chemistry* 286(14):12785-12795.
3. Kahsai AW, Rajagopal S, Sun J, & Xiao K (2014) Monitoring protein conformational changes and dynamics using stable-isotope labeling and mass spectrometry. *Nat Protoc* 9(6):1301-1319.
4. Xiao K*, et al.* (2018) Revealing the architecture of protein complexes by an orthogonal approach combining HDXMS, CXMS, and disulfide trapping. *Nat Protoc* 13(6):1403-1428.
5. Haas W*, et al.* (2006) Optimization and use of peptide mass measurement accuracy in shotgun proteomics. *Molecular & cellular proteomics : MCP* 5(7):1326-1337.
6. Bakalarski CE*, et al.* (2008) The impact of peptide abundance and dynamic range on stable-isotope-based quantitative proteomic analyses. *Journal of proteome research* 7(11):4756-4765.